CHAPTER 38

WAVES INDUCED BY NON-PERMANENT PADDLE MOVEMENTS

by C.Campos MORAES*
F.Silveira RAMOS**
M.Mendes de CARVALHO**

ABSTRACT

In a flume equipped with an irregular wave maker the motion of the paddle and the resulting waves may be thought of respectively as input and output of a system which, if linear, is for some purposes described by the so-called gain function.
A theoretical and experimental study of this function is carried out making use of paddle movements that produce transient surface motion.

1. INTRODUCTION

At the Laboratório Nacional de Engenharia Civil, a new flume was recently built for reproducing irregular (random) waves (fig.1). Length, width and depth of the flume are respectively 50, 1.60 and 1.20 m and the maximum water depth is 0.8 m. Waves are generated by the motion of a paddle actuated by a hydraulic jack, which is controlled, through a servo-valve, by an electrical signal of programmable characteristics, such as a given spectrum, if the signal is stationary, a given amplitude, if it is a sinusoid, etc. The structure linking paddle and actuator, a four-bar system, is such that the paddle may either be kept normal to the shaft of the actuator during motion (translation) or it may undergo a rotation as shown in fig. 1.

For the simulation of sea waves it is necessary to know the relationship between paddle motion and generated surface motion. For our purposes it is convenient to consider the flume a system for which input and output are respectively x(t), the (horizontal) displacement of the actuator shaft, and y(t), the water surface at a point, as functions of time. Of course, the system will be different for different water depths and for different positions of the points A and B in the four-bar structure that supports the paddle. In this paper, only the translation case is

* - Research Officer, Laboratório Nacional de Engenharia Civil, Lisbon, Portugal.
** - Trainee Research Officer, Laboratório Nacional de Engenharia Civil, Lisbon, Portugal.

considered and the water depth is 0.50 m, unless otherwise stated.
We assume that the system $\{x(t), y(t)\}$ is time-invariant. If it is also linear, we have

$$y(t) = h(t) * x(t) \tag{1}$$

where $*$ denotes convolution and h(t) is a function which characterises the system. If we put

$$G(f) = \left| TF\left[h(t)\right] \right| \tag{2}$$

where TF indicates Fourier transform, it is well known that
(i) if x(t) and y(t) are realisations of stationary stochastic processes with variance spectra $P_x(f)$ and $P_y(f)$, respectively, then

$$P_y(f) = G^2(f)P_x(f) \tag{3}$$

(ii) if x(t) and y(t) are transient functions, then

$$\left| TF\left[y(t)\right] \right| = G(f) \left| TF\left[x(t)\right] \right| \tag{4}$$

(iii) if x(t) and y(t) are sinusoids of frequency f_o and amplitudes A_x and A_y respectively, then

$$A_y = G(f_o)A_x \tag{5}$$

G(f) is the gain function of the system and $G^2(f)$ is sometimes called its transfer function.
Thus, if the system is reasonably linear and if we are able, as is the case, to control the characteristics of the input, a knowledge of G(f) will suffice to generate, for instance, waves with a given spectrum, $P_y(f)$.
A relationship of the form (5) for sinusoids has been obtained theoretically by Biésel & Suquet (1951), not for each frequency f but for each wave number, k. After adaptation for frequency, their formula is plotted in fig. 2. This relationship was derived using the linearised Hydrodynamics equations, a simplification we will also adopt.
Thus, apart from energy losses due to leakage around the paddle edges and the like, the problem of determining G(f) may be considered solved if for this purpose one may assume that the system $\{x(t), y(t)\}$ is linear, which allows the use of the formula not only for sinusoids but for any movements. This assumption may be studied theoretically making use of the solution by Kennard (1949) for the linearised equations of Hy-

drodynamics, precisely in the case of waves generated by paddle movements. One procedure is the following: a transient motion of the paddle and the corresponding surface profile at a point, computed by Kennard's formula, are considered; these are Fourier transformed and (4) is applied. The obtained G(f) is then compared with the one by Biésel & Suquet. If results are similar one may infer that in what concerns the determination of G(f) the linearity assumption for the system $\{x(t), y(t)\}$ is justified, at least as long as the linearised equations are applicable to water waves. Another procedure, this one with approximate results only, is based on the fact that, for a time-invariant linear system, if

$$x(t) = U(t) \tag{6}$$

where U(t) is the unit step function, that is, $U(t) = 1$ for $t > 0$ and $U(t) = 0$, for $t \leqslant 0$, then

$$h(t) = \frac{dy}{dt} \tag{7}$$

and so

$$G(f) = \left| TF\left[\frac{dy}{dt}\right]\right| \tag{8}$$

Kennard's solution does not allow the use of such an input. However, if instead of U(t) we use

$$\tilde{U}(t) = \begin{cases} 0 & , \quad t \leq 0 \\ \frac{t}{T} & , \quad t \in (0,T) \\ 1 & , \quad t \geq T \end{cases}$$

with T sufficiently small, then $\tilde{y}(t)$ being the resulting surface by Kennard's formula, we will have

$$G(f) \approx \left| TF\left[\frac{d\tilde{y}}{dt}\right]\right| \tag{10}$$

Similar and other procedures may be used for an experimental study in the flume using actual records of inputs and outputs instead of theoretical inputs and Kennard's outputs. This will permit to see not only whether the linearisation of the Hydrodynamics equations is too gross an approximation for our purposes, but also whether the linear assumption for the system is supported by experimental evidence. Experimental tests will also help in judging the accuracy of numerical integration necessary for Kennard's formula.

2. USE OF NON - PERMANENT PADDLE MOVEMENTS

We call non-permanent those paddle movements which produce transient surface motion. The importance of such movements in the determination of G(f) and the testing of the system linearity, as described above, results from several facts:

(i) with sinusoidal movements the system behaviour as regards linearity cannot be tested. Even assuming linearity, many flume experiments must be made to test the appropriateness of the B & S formula.

(ii) realisations of stationary stochastic processes have the drawback that spectra must be estimated from limited lengths of record.

(iii) non-permanent motions of the paddle are simpler to use with Kennard's formula especially those with constant absolute values of the velocity such as are shown in fig. 3, and which for lack of better names will be called "impulses" and "steps".

(iv) these impulses have simple Fourier transforms to apply in (4); the steps are such that it is simple to determine $\frac{d\bar{y}}{dt}$ for use in (10).

(v) tests in the flume, with such inputs are quite simple to perform and take little time.

3. THEORETICAL TESTS

3.1 - Theory

The two-dimensional surface profile for waves produced by the movements of a paddle is, as obtained by Kennard (1949) from the linearised Hydrodynamics equations and quoted by Madsen (1970),

$$\eta(x,t) = -\frac{2}{\pi}\int_0^{+\infty} dk \int_0^t d\tau \int_0^{-d} dz \; \frac{\cos\sigma(t-\tau).\cos kx.\cosh k(z+d)}{\cosh kd}\, u(z,\tau) \qquad (11)$$

where $\eta(x,t)$ is the surface elevation on time t and at distance x from the paddle, $\sigma = (gk \tanh kd)^{1/2}$, k being the wave number, d is the water depth and $u(z,\tau)$ is the horizontal velocity of the paddle on instant τ and on ordinate z. Of course, if there is no rotation, u is independent of z.

We will have then for a step

$$u(\tau) = \begin{cases} v \,, & \tau \in (0,T) \\ 0 \,, & \tau \notin (0,T) \end{cases} \qquad (12)$$

and for an impulse

$$u(\tau) = \begin{cases} v/2 \ , & \tau \in (0,T/2) \\ -\ v/2 \ , & \tau \in (T/2,T) \\ 0 \ , & \tau \notin (0,T) \end{cases} \tag{13}$$

where v = H/T.

After some manipulation, we obtain for the surface time profiles at distance x from the paddle

$$\eta_s(x,t) = \frac{4v}{\pi} \int_0^{+\infty} W(k,x) \cos \sigma(t - \frac{T}{2}) dk \tag{14}$$

$$\eta_i(x,t) = - \frac{8v}{\pi} \int_0^{+\infty} Q(k,x) \sin \sigma(t - \frac{T}{2}) dk \tag{15}$$

where subscripts s and i indicate step and impulse respectively, and

$$W(k,x) = \frac{1}{k\sigma} \tanh kd.\cos kx.\sin \frac{\sigma T}{2} \tag{16}$$

$$G(k,x) = \frac{1}{k\sigma} \tanh kd.\cos kx.\sin^2 \frac{\sigma T}{4} \tag{17}$$

The derivative of η_s is simple to obtain

$$\frac{d\eta_s}{dt} = - \frac{4v}{\pi} \int_0^{+\infty} W(k,x).\sigma.\sin \sigma(t - \frac{T}{2}) dk \tag{18}$$

The Fourier transform of the theoretical input impulse is in absolute value

$$A(f) = \frac{HT}{2} \left(\frac{\sin \pi f \frac{T}{2}}{\pi f \frac{T}{2}} \right)^2 \tag{19}$$

3.2 - Use of Kennard's solution

To have an experimental equivalent to the theoretical impulse to be used, a test was performed in the irregular wave flume with the experimental impulse shown in fig. 5. The width was the smallest that could be achieved by the actuator. In the manner of fig. 3, the values of H = 3.16 cm and T = 0.54 s were obtained for the "equivalent" theoretical impulse. As there were actual records from the flume at distances x = 5 m and x = 29 m from the paddle, Kennard's theoretical outputs were then computed by formula (15), for these distances, using Simpson's rule for the numerical integration. After some trials, the upper limit of integration and the step size were chosen to be 0.8 and 0.0005 respectively, the length unit being the centimetre.

Comparison of the theoretical (fig. 4) and the experimental (fig. 5) outputs for x = 5 m shows good agreement in periods and heights, except perhaps in the shorter periods towards the end. For x = 29 m agreement was still good in the longer periods but worse in the end as there was earlier dampening in the experimental record. This was ascribed to the numerical error in the integration and studies were confined to the x = 5 m case.

No comparison was made of surfaces produced by steps, as in the theoretical case there was no intermediate surface computation. The derivative of the surface was obtained instead by formula (18).

3.3 - The theoretical gain function

The function G(f) was computed by (4) for x = 5 m from the theoretical impulse mentioned in 3.2, that is, with H = 3.16 cm and T = 0.54 s. The Fourier transform of the corresponding Kennard surface profile was computed by the FFT algorithm. $\left|TF\left[x(t)\right]\right|$ is given by (19). G(f) values are plotted in fig. 6 (squares). G(f) was also computed by (10) for x = 5 m from a theoretical step with H = 1 cm and T = 0.05 s. $\frac{d\bar{y}}{dt}$ was obtained by (18) with a numerical integration similar to the impulse case. The Fourier transform was also computed numerically by the FFT algorithm and and the resulting G(f) values are plotted in fig. 6 (circles). It is seen that the G(f) values obtained by two procedures through Kennard's formula agree quite well with the Biésel-Suquet curve for translation which is also shown in fig. 6. The points resulting from the step (circles) show some dispersion, perhaps due to the fact that (10) is merely an approximative formula.

This good agreement seems to indicate that if the linearised Hydrodynamics equations are a sufficiently good approximation, then the system $\{x(t),\ y(t)\}$ may be taken as linear.

In the following section some experimental results are now presented.

4. EXPERIMENTAL TESTS

4.1 - Preliminary tests

For the determination of the gain function there had been some preliminary tests with sinusoids and white noise, that is, with permanent paddle movements. In what concerns spectral width, this corresponds to the use of two extremes: inputs with extremely wide and extremely narrow spectra.

Thus, for frequencies in the range of interest, that is, up to 2.0 cps, sinusoidal inputs of several amplitudes were used. The corresponding G(f) values, computed by (5), for x = 29 m are plotted in fig. 7. The scatter reveals that in practice there is some non-linearity in the system $\{x(t), y(t)\}$ in what concerns multiplication by a constant. However the overall agreement is good at least for $f \leq 1.5$ cps.

The white noise was provided by a white noise generator with an upper frequency limit of 1.5 cps(1), which is still within the range of interest. Nevertheless the test was made, input and output spectra were estimated and G(f) was computed by (3), also for x = 29 m, and plotted in fig. 7. What small energy there was in the input above 1.5 cps still provided some points for f>1.5 cps, which however should be viewed with some reserve, as according to Tick (1963), when computing the transfer function one should "use inputs that were rich in all frequencies of interest to obtain proper estimates".

The agreement between the two sets of points is good until $f \approx 1.3$ cps. Above this frequency the G(f) values obtained through white noise fall rapidly below the theoretical value of 2 cps. This may be due to two facts: (i)G(f) estimates are poor because of the 1.5 cps limitation of the available white noise; or (ii) there is in practice a lack of linearity which is specially felt above 1.3 cps. This seems to be related to the already mentioned differences between experimental and Kennard surfaces in the shorter periods and is probably caused by energy losses due to the variations of velocity and acceleration that occur in irregular waves.

4.2 - Experimental tests with non-permanent paddle movements for comparison with theory

In the experimental test referred to in 3.2, with an impulse (test nº.101) records were made at distances x = 5 m, x = 19 m and x = 29 m. G(f) was computed by (4) for the three distances. All Fourier transforms including that of the input were calculated numerically.

Results are shown in fig. 9.

---

(1) -In fact there were greater upper limits, but the next one available was 5 cps, already too high to use as input for the actuator.

Let us consider for the moment only the 29 m G(f) values. It is seen that the experimental values while showing reasonable agreement until f ≈ 1.6 cps then fall well below the theoretically obtained ones. It should be noted that theoretically and in practice the input energy will not reach zero values before about 4 cps and that at 2 cps the input energy is still about 40 percent of its maximum. Thus it seems that the fall in G(f) values is real, above 1.6 cps, that is, it must be explained at least in part by a lack of linearity in the higher frequencies. Results from the experimental step shown also in fig. 5 were not good enough. The derivative of the function represented by the record was computed and then Fourier transformed to obtain an approximation of G(f) according to (10). Results, shown in fig. 8, were not good, probably because the width T = 0.27 s of the step was too large, although it was the smallest the equipment could produce. The theoretical step, which gave reasonable results, had one fifth of the width.

4.3 - Tests with non-permanent movements for studying the influence of certain parameters on the experimental gain function

4.3.1 - Variation along the flume

Fig. 9 shows the variation along the flume of the gain function G(f) as computed from records made at 5 m, 19 m and 29 m from the paddle in test no. 101 (fig. 5). There is a distinct dampening of G(f) as x increases which may be ascribed to energy losses in the wave propagation. The absolute values of the Fourier transform F(f) of the surface profile at each one of the three distances is shown in fig. 10. Another feature is the overshooting of experimental G(f) values at 5 m above the theoretical ones in the range 1.1-1.9 cps. This may possibly have one or both of the following explanations: (i) there is still turbulence in the surface at 5 m from the paddle in this case; (ii) on the one hand the B & S formula is not so well verified in practice, but on the other hand the energy loss along the flume is such that at 19 m and 29 m it brings down the G(f) values in a way which makes them approximate the theoretical curve. This needs further investigation.

4.3.2 - Variation with impulse parameters

Besides the experimental impulse of test no. 101, other experimental tests were made with impulses with different values of H and T. In table 1, these tests are summarised.

This table shows that the impulses of tests 102, 103 and 104 are proportional to that of test 101 and so if the system $\{x(t), y(t)\}$ is linear then the resulting surface profile should be the same, only with a different scale of elevation. That this was indeed approximately so is reflected in the fact that variations in the corresponding G(f) values are but small, fig. 11.

Table 1 - Experimental impulse inputs used

Test no.	H (cm)	T (s)
101	3.16	0.536
102	2.46	0.536
103	2.05	0.536
104	1.62	0.536
105	3.54	0.760
106	3.98	1.04
107	4.00	1.36
108	3.91	1.76

The result of using impulses with successively larger T, as in tests 101, 105, 106, 107 and 108 is shown in fig. 12. The larger the T, the sooner the fall in the G(f) values. This is explained by the fact that wide impulses are poorer in the higher frequencies. In fact it can be shown that the impulse input energy falls down to zero when f reaches the value $\frac{1}{2T}$. This value is about 4, 2.6, 2.0, 1.5, 1.1 cps, respectively, for the five tests, and it is seen that the last three are still within the frequency range of interest. On the other hand, while the zero value for the impulse of test no. 101, which had the smallest width possible, is not reached before 4 cps, the G(f) curve is still below the theoretical curve for $f > 1.6$ cps and so, lack of linearity seems to play a part in this fall; it would be interesting to see curves for narrower experimental impulses if it were possible to obtain them, which it is not, owing to mechanical and hydraulic limitations.

4.3.3 - Variation with water depth

As mentioned in the introduction, the water depth used for all the tests described was 0.50 m. However, tests with impulses similar to that of test no. 101 have also been made for other depths. Fig. 13 shows G(f) computed by (4) for x = 29 m and for depths d = 0.20, 0.30, 0.40, 0.50 and 0.80 m. The B & S curves for 0.20, 0.50 and 0.80 m are also indicated for comparison.

Non-linearity is apparent at all depths especially at the shallower ones, where deviation of experimental G(f) values from B & S curves is evident at all frequencies. Thus for each surface spectrum to be used in tests, the corresponding input will probably have to be determined by successive approximations, possibly starting with the experimental G(f) obtained through the use of a narrow impulse input.

In the higher depths there is however a reasonable agreement between experimental G(f) points and the B & S curves in the lower frequencies, that is, the system may be considered for these frequencies as approximatively linear. In fact, d'Angrémond & Van Oorschot (1969) report good results using the B & S curves for a depth of 0.40 m. The spectra they used had only a small percentage of their energy out of the range where for that depth non-linearity is more strongly felt. It is interesting to note, however, that they also report somewhat lower values than expected in the output spectra for the higher frequencies, which is in accordance with the fall observed in all experimental G(f) values after 1.5, 1.6 cps.

5. CONCLUSIONS

A summary of the more important conclusions drawn in preceding sections is:

- The linearised equations of Hydrodynamics from which the B & S curves were derived for sinusoidal movements imply that the system $\{x(t), y(t)\}$ is linear and so those theoretical curves should apply even for non-sinusoidal movements whenever the linearised equations are a good model for water waves. In practice it was found that non-linearity of the system was present at all depths especially at the shallower depths and higher frequencies. However, in many cases where higher depths and lower frequencies, only, are of interest it is to be expected that the mentioned non-linearity will not prevent the validity of the use of an approximate gain function possibly coincident with the ascending branch of the B & S curves.

- In what concerns variation along the flume a slight decrease in the wave energy was detected as distance from the paddle increased.
- Non-permanent paddle movements of the impulse type were found to be quite convenient for these gain function studies both for use with Kennard's formula and for experimental tests. As expected narrower impulses produce better results and so the narrowest impulses compatible with mechanical and hydraulic limitations should be used.

6. BIBLIOGRAPHY

1. BIÉSEL, F. and F. SUQUET - Les appareils générateurs de houle en laboratoire, La Houille Blanche, nos. 2, 4, 5 - 1951, 6 - 1952.

2. D'ANGREMOND, K. and J.H. VAN OORSCHOT - Generation of irregular waves on model scales, Proceedings of the Symposium Research on Wave Action, Delft Hydraulics Laboratory, Delft, the Netherlands, 1969.

3. KENNARD, E.H. - Generation of surface waves by a moving partition, Quarterly of Applied Mathematics, vol. 7, No. 3, 1949.

4. MADSEN, O.S. - Waves generated by a piston type wavemaker, Proceedings of the Twelfth Coastal Engineering Conference, Washington, 1970.

5. TICK, L.J. - Conditional Spectra, Linear Systems and Coherency, Proceedings of a Symposium on Time Series Analysis, edited by M.Rosenblatt, John Wiley and Sons, Inc, New York, 1963.

6. DAS, M.M. and R.L.WIEGEL - Water waves generated by horizontal motion of a vertical wall, Tech. Rep. HEL 16-7, University of California, Hydraulic Engineering Laboratory, Berkeley, 1971.

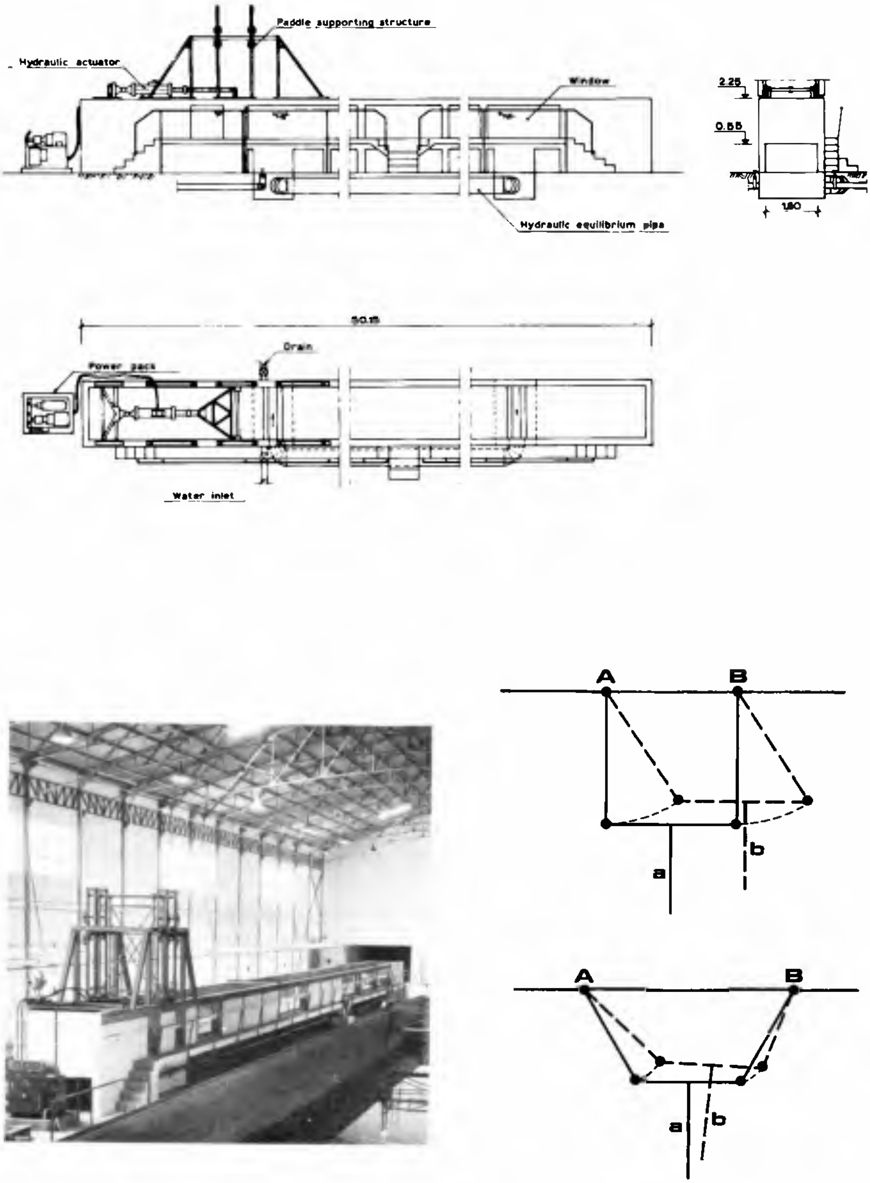

Fig. 1 - Irregular wave flume

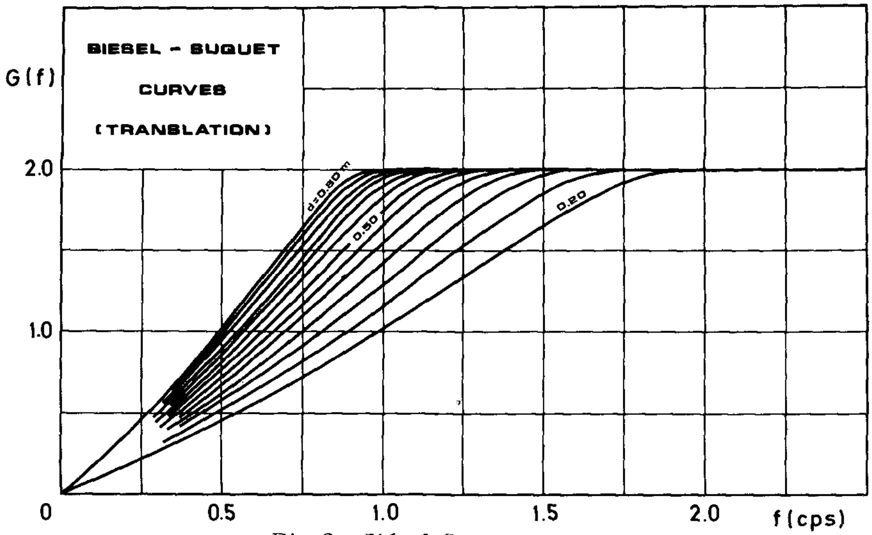

Fig. 2 - Biésel-Suquet curves

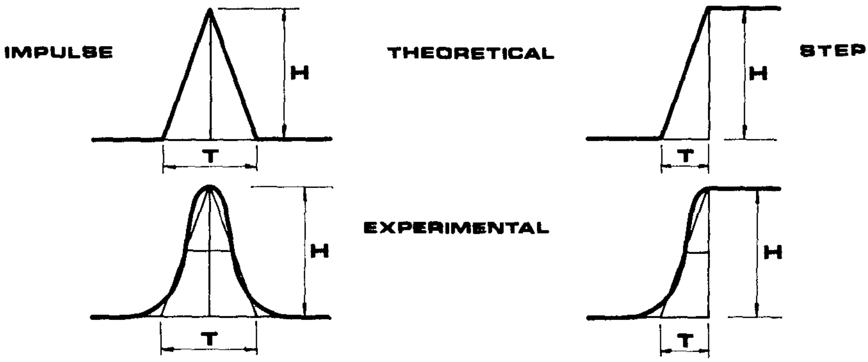

Fig. 3 - Definition sketch for impulses and steps

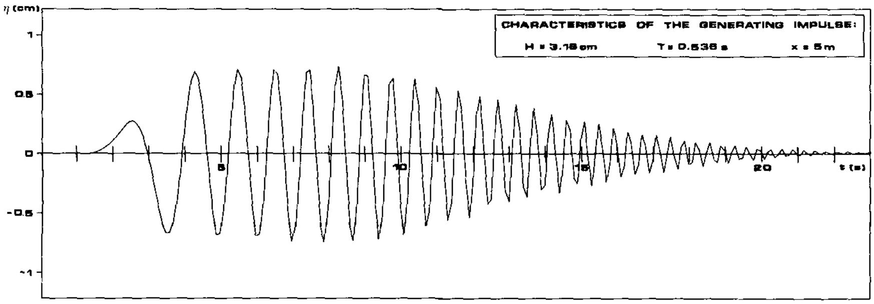

Fig. 4 - Kennard surface profile generated by an impulse

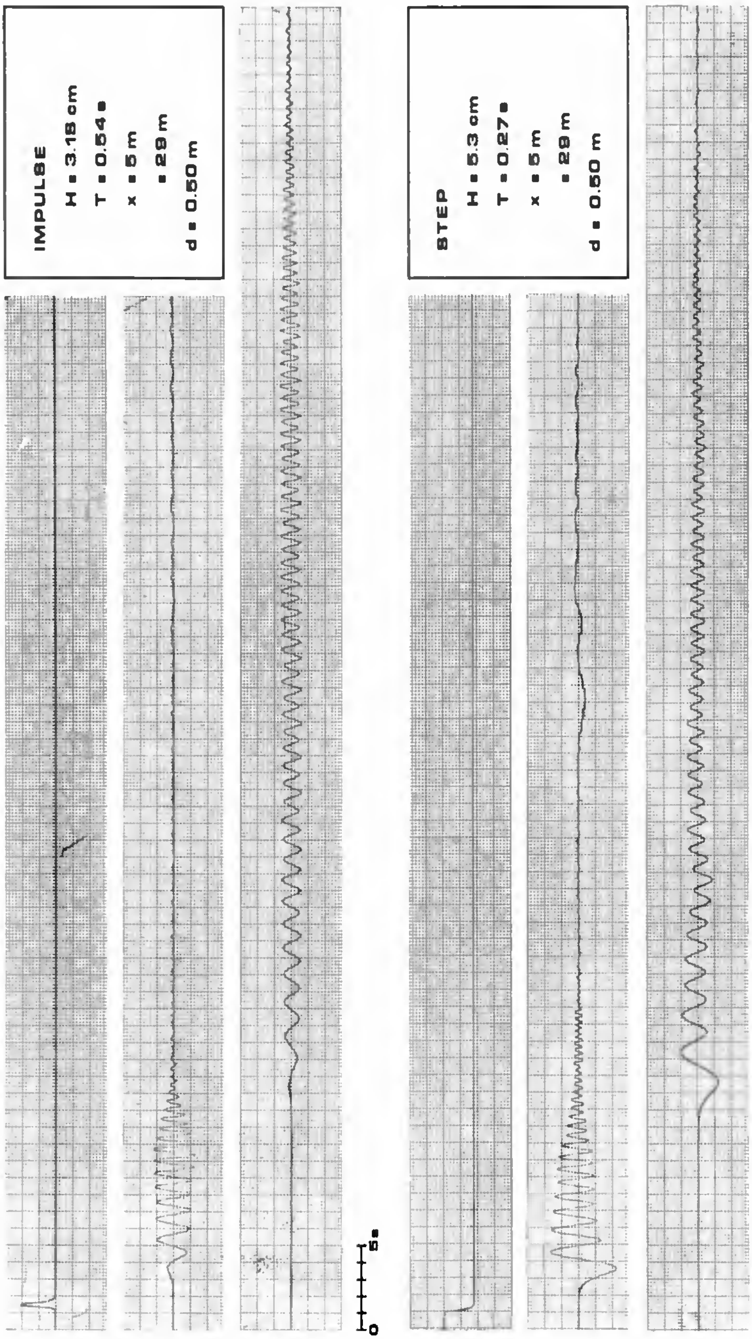

Fig. 5 - Experimental impulse and step and corresponding records

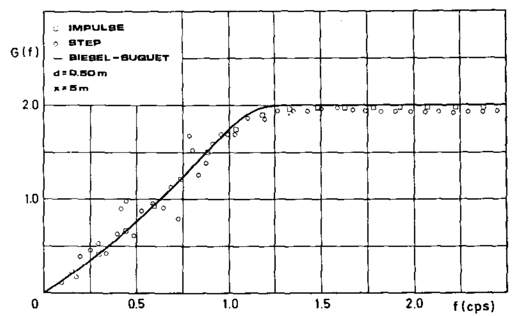

Fig. 6 - Theoretical gain functions from impulse and step compared with Biésel-Suquet curve

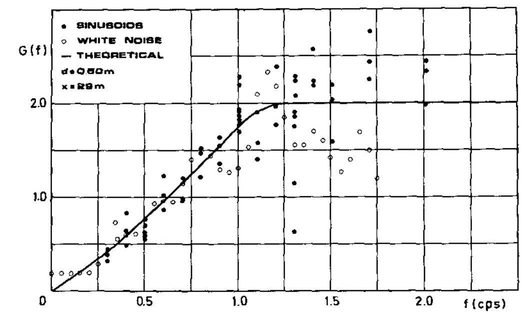

Fig. 7 - Experimental gain functions from sinusoids and white noise

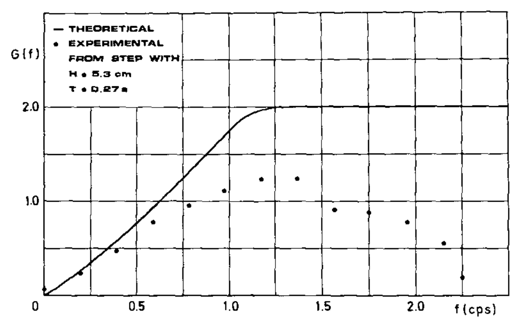

Fig. 8 - Experimental gain function from step

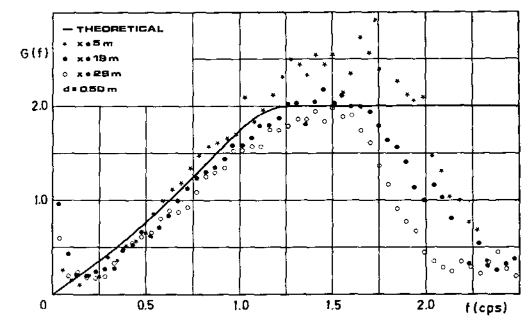

Fig. 9 - Variation of experimental gain function along the flume

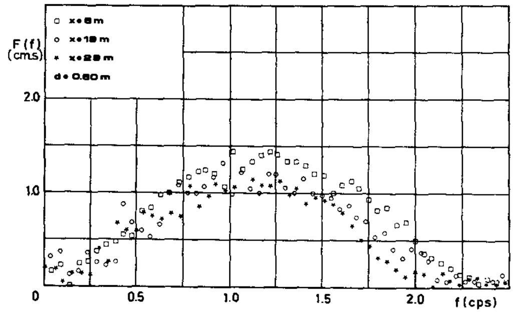

Fig. 10 - Variation of experimental surface Fourier transform along the flume

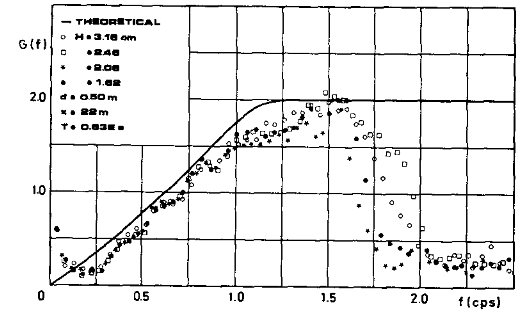

Fig. 11 - Variation of experimental gain function with impulse height

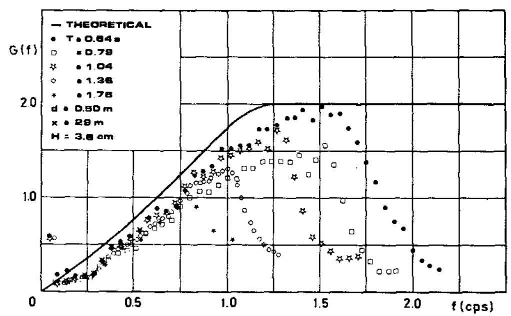

Fig. 12 - Variation of experimental gain function with impulse width

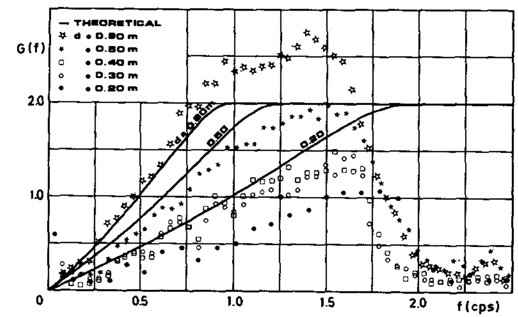

Fig. 13 - Variation of experimental gain function with water depth